Sonic velocity and grain contact properties in reservoir sandstones

Vidar Storvoll and Knut Bjørlykke
University of Oslo, Department of Geology, PO Box 1047 Blindern, N-0316 Oslo, Norway
(e-mail: vidar.storvoll@geologi.uio.no)

ABSTRACT: The purpose of this study was to examine the effect of grain contacts and quartz cementation with regard to acoustic wave propagation in sandstones. Grain contacts have been considered essential when relating acoustic velocities to physical rock properties, and a parameter numerically representing the contact area between individual grains (contact length) has been measured. The method used involves digital petrographic microscopy pictures analysed by image analysis software. Other parameters, such as grain size, number of grain-to-grain contacts, cracks, clay content and porosity, have also been closely examined. The results showed that the contact area between sand grains may be useful for explaining velocity variations during the initial stages of quartz cementation and grain framework stiffening. Continued increase in grain-contact area by chemical compaction will have less influence on the sonic velocity compared to variations in porosity. The Garn Fm. from the Norne Field (2.6–2.7 km burial depth), which is in the early phase of initial grain framework stiffening by quartz cementation, and the Garn Fm. from the Kristin Field (4.6–4.7 km burial depth), which is thoroughly quartz cemented, were chosen as sample materials. Log-derived velocities, in addition to some laboratory ultrasonic velocity measurements, were used in this study.

KEYWORDS: *sandstones, cementation, contact area, elasticity, sonic velocity*

INTRODUCTION

Several studies have pointed out the significance of grain contacts in relation to acoustic velocities in sandstones (e.g. Love 1927; Mindlin 1949; Digby 1981; Walton 1988; Anstey 1991; Dvorkin *et al.* 1991; Nur *et al.* 1991), but satisfactory quantitative relationships are still not established. Simplistically stated, the basic idea is that thoroughly cemented sandstones have many and large grain-to-grain contacts and are, therefore, stiffer, with higher sonic velocities compared to sandstones with minor amounts of cement, fewer contacts and small contact areas.

Bernabé *et al.* (1992) and Wang (2000) stated that it is very difficult to use real geological core samples and *in-situ* well measurements when studying single micro-mechanical parameters in sedimentary rocks. Very few attempts have, however, been made both because of the obvious theoretical difficulties and because a practical method has been absent.

Rigidity, bulk modulus, shear modulus, Poisson's ratio and impedance are parameters often used instead of velocity when working with rock physics and elasticity in rocks. V_p, V_s and density have, however, been preferred in the results and discussion throughout this paper, with only a few exceptions. The rock modulus and other rock physic parameters can be expressed through combinations of V_p, V_s and density. When using the term 'velocity', the paper refers to both compressional and shear velocity, if not stated otherwise.

By using core samples and well logs representing *in-situ* reservoir conditions, the intention was to test numerically the relationship between sonic velocity and grain contact parameters. A few samples also underwent laboratory ultrasonic velocity analysis. A method was developed to measure quantitatively a parameter representative for the actual area in grain-to-grain contacts. Grain size, number of grain-to-grain contacts, cracks, clay content and porosity were also considered with regard to the observed velocity variations.

BACKGROUND

Sonic velocities in sedimentary rocks are affected by numerous geological factors, including mineralogy, porosity, pore and grain geometry (aspect ratio), pore fluid, clay content, bulk density, effective stress, type and degree of cementation (diagenesis), degree and orientation of cracks, grain size, sorting, number of grain-to-grain contacts per grain, pore pressure, confining pressure, temperature, velocity anisotropy, contact stiffness and contact size (Wyllie *et al.* 1956, 1958; Nur & Simmons 1969; Winkler 1983; McCormack *et al.* 1985; Lo *et al.* 1986; Murphy *et al.* 1986; David *et al.* 1988; Nur & Wang 1989; Anstey 1991; Bernabé *et al.* 1992; Vernik 1998; Wang 2000). Many of these factors influence each other and, according to Bernabé *et al.* (1992), it is practically impossible to separate the effect from one factor with regard to rock strength. At least it is impossible to assess the effect of one factor without considering the effects from others (Wang 2000).

Experimental studies have found relatively clear relations between seismic velocities, porosity and clay content (Wyllie *et al.* 1956, 1958; Han *et al.* 1986; Vernik & Nur 1992). Nur & Wang (1989) found that velocity is approximately three times more sensitive to porosity than clay content, while Klimentos (1991) found it twice as sensitive. The distribution of clay particles (e.g. laminated clay or clay in the matrix) is more

important than the volumetric amount of clay in the rock. Clay has a tendency to reduce the shear modulus to the rock matrix and the shear velocity will experience a more significant velocity reduction than the compressional velocity. The V_p/V_s ratio will exhibit a general increase (Miller & Stewart 1990).

Mechanical compaction starts right after deposition and is driven by the vertical stress from the increasing overburden. The process involves sliding, reorientation, bending, ductile deformation and crushing of grains, making the grain framework more rigid. Chemical compaction involves dissolution and precipitation of minerals and is mainly controlled by temperature. The most important type of chemical compaction in reservoir sandstones is precipitation of quartz, which begins at 70–80°C (Bjørlykke *et al.* 1986; Ehrenberg 1990; Walderhaug 1994). The volume of quartz cement and subsequent reduction in porosity, however, is a function of the temperature integrated over time (Walderhaug, 1996, 2000; Bjørkum *et al.* 1998).

It has been shown that even small amounts of cement at the grain contacts will significantly increase the stiffness and, thereby, the velocity, of a granular material by preventing gliding or rotation between the grains (Winkler 1983; Bernabé *et al.* 1992; Vernik & Nur 1992; Dvorkin & Nur 1996), even if the cement is relatively soft (Dvorkin *et al.* 1994). This means that it is the actual distribution of cement in the samples that is critical, not the bulk volume cement (Bernabé *et al.* 1992; Dvorkin *et al.* 1994). The initial cementation also reduces the effective stress per grain contact, both by increasing the contact area and number of grain-to-grain contacts. This explains why mechanical compaction and grain crushing rapidly ends after the onset of quartz cementation (70–80°C). The severe textural changes in the grains and grain contacts that are caused by mechanical and chemical compaction suggest that it is more appropriate to consider grain contacts as an area rather than point-to-point contacts.

The aspect ratio of a pore or crack is a measure of its flatness and is defined as the ratio of the minor to major semi axis of a spheroid (Wilkens *et al.* 1984). Xu & White (1995, 1996) argue that pore geometry (pore aspect ratio) can explain most of the scatter in the porosity–velocity relationships and Tao & King (1993) state that pore structure is one of the most important, but often neglected, factors that influence sonic velocities in rocks. In relatively pure sandstones velocities are very sensitive to the presence of thin cracks and crack-shaped or flat pores (aspect ratio $\ll 1$), especially if the thin pores are aligned (the rock becomes anisotropic). Cracks in grains will, however, be the first areas to become cemented after the onset of quartz cementation (Xu & White 1995; Walderhaug 1996; Fisher & Knipe 1998; Chuhan *et al.* 2002), mainly because clean mineral surfaces will have excellent nucleation positions making it easier for quartz to precipitate. Pores with low aspect ratios will also become 'separated' more easily or 'divided' into several individual pores by cementation when compared to more circular high aspect ratio pores. This implies that, with increasing burial, the presence of cracks and low aspect ratio pores will be significantly reduced and velocity will be less influenced by pore shape.

EXPERIMENTAL PROCEDURE

Sample material

Core samples, well logs, fluid composition and other data necessary were provided by Statoil ASA. All sample and well-log measurements are given in core depth (mRKB). Relatively pure sandstones were chosen as samples to minimize the important effect of varying clay content. Samples from the Garn Fm. in the Kristin (well 6406/2-3T3) and Norne (well 6608/10-2) fields have been studied. The Kristin Field stretches over Block 6406/2 and 6506/11 and is located approximately 220–230 km offshore Mid-Norway. The Norne Field is located approximately 180 km offshore Mid-Norway, 160 km NE of the Kristin Field and extends into Blocks 6508/1 and 6608/10. All the samples have been buried deeper than the onset of quartz cementation (70–80°C). The Kristin samples are from 4.6–4.7 km depth, corresponding to approximately 160°C (Storvoll *et al.* 2002), have a medium grain size (average of 0.35 mm) and are thoroughly cemented (Table 1). The samples from the Norne Field are located between 2.6 km and 2.7 km (approximately 90–100°C, assuming a temperature gradient of 35–40°C km^{-1}), have a very fine to fine grain size (average of 0.12 mm) and small amounts of quartz cement (Table 1). Quartz cement is the main diagenetic mineral in the sample sets, but carbonate-cemented intervals are also common, especially in the Norne samples. Other diagenetic minerals like pyrite are not quantitatively significant. The Garn Fm. is interpreted as a subarcosic arenite.

Methods

Pictures (dimension of 1.4×1.9 mm) with normal transmitted light and x-nicols from five locations on each thin section were taken with a digital camera mounted on a transmitted light microscope. The five pictures are located along a straight line perpendicular to the layering of the sample with equal distance between each picture relative to the size of the sample. A scale bar was also photographed for each thin section to see how many pixels correspond to a fixed length after downloading the pictures to the computer, regardless of camera and microscope settings. This was also necessary to calibrate the measurements in the image analysis software, SigmaScanPro4 (1995) from Jandel Scientific and to transform the data to a common unit, making correlation between the samples possible. Each picture often contained more than 300 grain contacts (depending on grain size, sorting, cementation etc.), which could result in average grain contact measurements based upon 1500 contacts for each thin section. Grain size and number of grain-to-grain contacts per grain were also measured. These averaged values are both based upon a minimum of 50 grain measurements for each thin section. A scanning electron microscope (SEM) with a cathodoluminescence (CL) detector was used to further study the grain contacts, cracks and quartz cementation.

The effect of variable hydrocarbon saturation was eliminated from the sonic logs by bringing the entire dataset to a common pore fluid saturation (100% brine saturated). The fluid substitution was performed by following two procedures: (1) Gassmann's equation; and (2) the 'Mavko–Gassmann V_p only' method (Mavko *et al.* 1995). Both procedures consist of three steps: (1) use well-log data to calculate the elastic modulus of the dry rock; (2) use the dry-rock elastic moduli obtained and calculate the common-fluid rock modulus (K_c and M_c) for the entire interval; (3) use the common-fluid rock modulus to calculate velocity and impedance as needed. The fluid and rock parameters used to perform the fluid corrections are listed in Table 2. The fluid-corrected velocity based on Gassmann's equation is referred to as $V_p(K_c)$ and are listed in Table 1. Shear waves are more or less unaffected by fluid content and no correction is necessary.

A total of 11 samples (five from the Norne well and six samples from the Kristin well) underwent ultrasonic velocity measurements at the Center for Rock Physics, University of Oklahoma (USA) on a fully automated velocity system based on a conventional pulse transmission technique (Schreiber *et al.* 1973). The transducers measured one compressional wave and

Table 1. *Data of the samples used in the study.*

Well	Core depth m	Contact length mm^{-1}	Grain contacts #	Grain size mm	He-porosity %	Density-porosity %	NPHI v/v	Gr GAPI	RHOB $g\,cm^{-3}$	V_p $m\,s^{-1}$	V_s $m\,s^{-1}$	Bulk moduli (K_c) GPa	Compressional moduli (M_c) GPa	Rigidity (μ) GPa	Poisson's ratio (σ)	$V_p(K_c)$ $m\,s^{-1}$	$V_p(K_c)/V_s$
6608/10-2	2622.40	2.26	1.80	0.111	26.3	21.6	0.239	50.82	2.24	3105.1	1807.2	16.10	27.14	7.33	0.30	3395.3	1.88
6608/10-2	2623.15	2.46	1.70	0.109	27.0	24.7	0.250	49.81	2.19	3215.3	1870.4	16.39	27.84	7.65	0.30	3487.2	1.86
6608/10-2	2640.40	3.21	1.95	0.102	28.5	25.1	0.261	43.89	2.18	3135.2	1818.2	15.80	26.58	7.20	0.30	3415.3	1.88
6608/10-2	2641.15	4.19	1.60	0.071	26.5	24.2	0.254	46.56	2.20	3171.5	1844.4	16.12	27.29	7.47	0.30	3446.5	1.87
6608/10-2	2642.40	1.49	2.07	0.141	29.1	19.9	0.248	51.78	2.28	3168.0	1845.6	16.51	28.11	7.75	0.30	3434.6	1.86
6608/10-2	2643.40	1.91	2.07	0.141	29.6	25.0	0.269	35.84	2.18	3277.1	1921.1	16.37	28.23	8.04	0.29	3526.2	1.84
6608/10-2	2647.75	2.02	2.24	0.142	29.2	26.2	0.256	35.96	2.16	3172.9	1847.4	15.84	26.81	7.36	0.30	3448.7	1.87
6608/10-2	2663.75	1.85	2.15	0.137	26.2	24.2	0.252	48.75	2.19	3179.5	1850.7	16.30	27.59	7.52	0.30	3463.2	1.87
6608/10-2	2670.25	2.37	1.93	0.115	27.9	23.5	0.257	46.12	2.21	3195.1	1851.3	16.32	27.64	7.57	0.30	3458.3	1.87
6608/10-2	2672.00	2.84	2.39	0.140	31.0	27.9	0.263	37.83	2.13	3145.7	1827.9	15.43	25.98	7.10	0.30	3422.6	1.87
6406/2-3T3	4634.34	3.30	3.90	0.337	16.3	16.2	0.130	12.46	2.31	3786.8	2598.9	18.88	40.22	15.63	0.18	4143.2	1.59
6406/2-3T3	4635.39	1.84	3.87	0.427	16.4	18.0	0.092	11.29	2.26	3916.1	2687.3	19.19	41.52	16.30	0.17	4249.1	1.58
6406/2-3T3	4636.11	2.48	3.48	0.389	14.9	13.1	0.114	9.40	2.38	3866.4	2627.3	20.04	42.64	16.41	0.18	4198.6	1.60
6406/2-3T3	4637.44	2.04	3.77	0.455	17.1	9.6	0.136	10.70	2.45	3877.5	2658.9	19.45	42.86	17.33	0.16	4166.9	1.57
6406/2-3T3	4638.25	2.49	3.73	0.428	16.0	8.0	0.096	10.83	2.48	3897.1	2678.5	19.89	43.96	17.82	0.16	4192.1	1.57
6406/2-3T3	4639.50	4.23	4.29	0.254	14.5	15.4	0.149	13.31	2.33	4118.0	2816.5	20.82	45.93	18.49	0.16	4417.4	1.57
6406/2-3T3	4645.34	2.51	3.95	0.420	15.4	13.7	0.120	11.45	2.37	3984.7	2745.3	19.96	44.00	17.84	0.15	4296.4	1.56
6406/2-3T3	4657.36	1.70	3.99	0.483	14.3	9.8	0.142	14.28	2.45	4071.0	2664.0	22.33	46.83	17.36	0.19	4311.4	1.62
6406/2-3T3	4658.35	2.82	3.34	0.298	17.7	13.7	0.140	16.38	2.37	3917.1	2576.7	20.29	42.25	15.70	0.19	4175.1	1.62
6406/2-3T3	4662.43	3.03	3.46	0.295	15.9	9.0	0.148	12.97	2.46	3891.7	2538.2	21.18	43.65	15.87	0.20	4145.3	1.63
6406/2-3T3	4678.00	3.55	3.92	0.285	13.4	12.3	0.124	11.82	2.40	4116.9	2770.8	21.82	47.21	18.39	0.17	4398.7	1.59
6406/2-3T3	4679.80	3.82	3.87	0.272	14.6	12.2	0.119	11.51	2.40	4093.7	2717.7	21.75	46.39	17.70	0.18	4350.1	1.60
6406/2-3T3	4682.00	2.88	3.99	0.313	14.9	12.1	0.114	10.90	2.40	4104.5	2749.2	21.49	46.50	18.14	0.17	4362.4	1.59
6406/2-3T3	4683.00	3.12	4.28	0.280	14.4	12.4	0.126	10.46	2.39	4354.8	2919.6	22.74	50.61	20.39	0.15	4568.4	1.56
6406/2-3T3	4686.00	3.36	4.65	0.368	12.7	10.3	0.097	11.42	2.44	4269.7	2863.8	22.96	50.48	19.98	0.16	4512.3	1.58
6406/2-3T3	4693.66	2.67	3.92	0.359	13.9	12.0	0.102	11.05	2.40	4147.2	2774.3	22.00	47.57	18.49	0.17	4407.2	1.59
6406/2-3T3	4696.00	2.90	3.64	0.327	15.0	11.8	0.119	11.39	2.41	4204.7	2796.0	22.18	48.15	18.81	0.17	4432.1	1.59
6406/2-3T3	4698.48	4.23	4.00	0.324	15.3	12.3	0.124	11.87	2.40	4171.2	2784.9	21.78	47.37	18.58	0.17	4407.9	1.58
6406/2-3T3	4701.25	3.01	4.08	0.403	13.5	11.8	0.097	9.56	2.41	4167.0	2847.5	21.63	48.10	19.51	0.15	4449.4	1.56

NPHI, neutron porosity log; Gr, gamma log; RHOB, density log; V_p and V_s values are from the sonic log; saturation and fluid type were taken into account when estimating rigidity, Poisson's ratio, bulk modulus and compressional modulus; $V_p(K_c)$ is derived from the common-fluid bulk modulus; contact-length unit (mm^{-1}) is explained in the text.

Table 2. *Fluid and rock parameters used in fluid correction*

	P MPa	T °C	$K_{mineral}$ GPa	$M_{mineral}$ GPa	K_{brine} GPa	K_{oil} GPa	K_{gas} MPa	K_{cond} GPa
Kristin	90.0	165.0	38	96.7	2.9			0.3953
Norne	25.1	98.4	38	96.7	3.6	1.0	58.8	

All the values listed refer to reservoir conditions; the hydrocarbons in the Garn Fm. from the Kristin Field are a condensate (or supercritical fluid); the bulk modulus for the brine, oil and gas in the Garn Fm. from the Norne Field were estimated from curves published in Batzle & Wang (1992).

two orthogonally polarized shear waves. The shear waves presented in this paper are the average velocity of the two polarized waves (Table 3).

Grain contact-length analysis

Before starting with the actual measurements it is important to get an overview of the sample, mineralogy, estimate approximately how much and which types of cement are present, and type of contacts that are to be measured by using a light microscope. After taking the necessary pictures and importing them to the image analysis software, the length of the contacts between all the grains in the five pictures from each thin section were measured. The number of pixels per millimetre in each picture may vary due to variations in microscope and camera settings. The total grain contact length (mm) for each picture (five pictures per thin section) was, therefore, divided by the area (mm^2) of the picture in question, before again averaging the five values for each thin section. This results in a unit of mm^{-1} for the contact-length measurements, which is used to numerically *represent* the contact area between the grains.

It is most practical to consider and define the shortest/smallest contact between two adjacent grains at the time (Fig. 1). It is common to find 'impure' grain contacts with some clay or altered minerals located between, or partly between, the grains. It is not correct to interpret this as an ordinary grain-to-grain contact because clay in the grain framework reduces the stiffness (especially the rigidity) and, thereby, velocity, but neither is it correct to ignore these contacts when doing the analysis. The grain framework will obviously be stiffer with some clay in the contacts than if no contact was present at all. To try and compensate for this problem only half the distance of the contacts influenced by clay was drawn up.

Contacts, in general, are seldom perfect continuous mineral–mineral boundaries even if no clay is present and patches/holes are often found along the contacts. It may also be difficult to determine the exact boundaries between grains in quartz-cemented samples and to separate cement from clastic grains when no 'dust line' around the grain is present. It is necessary to consider both the picture with normal transmitted light and the one with crossed nicols when performing the analysis. It is, however, important to do the actual measurements on the picture with normal transmitted light and not on the picture with crossed nicols since the double refraction makes the grains and contacts look bigger than they actually are. Examples of interpreted thin sections are shown in Figure 2.

RESULTS

All the log values and measured parameters for the studied samples are listed in Table 1. The deeply buried samples from the Kristin well (4.6–4.7 km) show a negative correlation between porosity and log-derived velocity (Fig. 3a). No correlation between porosity and velocity was found in the Norne well (Fig. 3b), where the Garn samples have undergone a much shallower burial (2.6–2.7 km). A number of grain-to-grain contacts shows a positive correlation with grain size in the Norne well (Fig. 3d), as a result of the transport processes active during deposition. In the Kristin well there is no correlation between these two parameters (Fig. 3c). A positive correlation between the number of grain-to-grain contacts and velocity was, however, found (Fig. 3e). The samples from the Kristin well also show a negative correlation between the number of grain-to-grain contacts and porosity, while the Norne samples show a positive trend between the two parameters (Figs 4a, b). Porosity should be expected to decrease when the number of grain-to-grain contacts increases, which indicates that the number of grain-to-grain contacts and porosity in the Norne samples are both controlled by other parameters. The GR-log reflects the total amount of clay in the samples and Figure 4d shows that porosity decreases with increasing clay content in the Norne well. It might also seem

Table 3. *Data used in the ultrasonic velocity analyses*

Well	Core depth m	P (DRY) $m\,s^{-1}$	S (DRY) $m\,s^{-1}$	P (WET) $m\,s^{-1}$	S (WET) $m\,s^{-1}$	Grain density $g\,cm^{-3}$	Dry density $g\,cm^{-3}$	phi %	K_{inf} mD	K_{air} mD
6608/10-2	2622.40	3247.0	1869.5	3525.0	1801.5	2.67	1.92	25.26	74.7	81.7
6608/10-2	2641.15	3343.0	2025.5	3390.0	1981.5	2.64	1.92	24.97	79.0	84.9
6608/10-2	2642.40	3184.0	1825.5	3461.0	1751.5	2.66	1.82	29.14	1290.0	1300.0
6608/10-2	2670.25	3086.0	1956.5	3309.0	—	2.66	1.92	25.42	159.0	165.0
6608/10-2	2672.00	3332.0	1936.0	3558.0	1842.5	2.67	1.86	27.84	784.0	795.0
6406/2-3T3	4634.34	4476.0	2899.5	4587.0	2825.5	2.66	2.25	14.27	39.6	42.2
6406/2-3T3	4636.11	4675.0	2861.0	4847.0	2833.5	2.65	2.25	13.94	81.4	86.3
6406/2-3T3	4639.50	4452.0	2665.5	4598.0	2615.0	2.67	2.29	12.96	0.3	0.3
6406/2-3T3	4686.00	4793.0	3091.0	4830.0	3016.5	2.65	2.45	11.56	0.2	0.3
6406/2-3T3	4696.00	4693.0	2833.5	4741.0	2757.0	2.66	2.27	13.52	1.3	1.6
6406/2-3T3	4698.48	4549.0	2905.0	4669.0	2835.5	2.66	2.27	13.61	0.5	0.7

The ultrasonic velocity analyses were performed at the Center for Rock Physics, University of Oklahoma (USA). The compressional (P) and shear (S) velocities shown were measured under wet and dry conditions at an effective pressure of 4000 psi. Density, helium porosity (phi) and permeability (K) measurements performed during the core analysis are also listed. The core plugs used in the ultrasonic velocity analysis are not the same as used when obtaining the data listed in Table 1. They are, however, sampled from the same cores and depths as indicated in the tables. The data are provided by Statoil ASA.

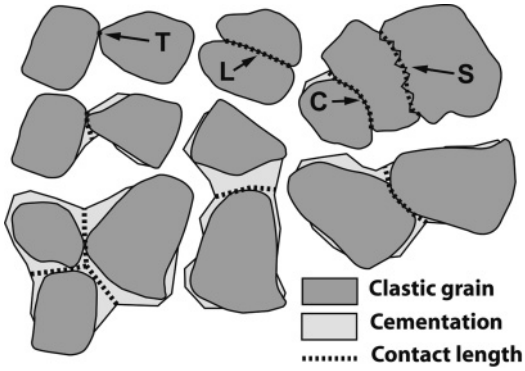

Fig. 1. Schematic illustration of how the contact length has been measured between grains undergoing varying degrees of compaction and cementation. The arrows show tangential (T), long (L), concavo-convex (C) and sutured (S) principal contacts (Taylor 1950) typically found in sandstones.

that a weak positive trend between clay content and porosity exists in the samples from the Kristin well (Fig. 4c). When plotting total amount of clay (GR-log) versus velocity (Figs 4e, f), no correlation or trend is found for either well.

The contact-length measurements (Fig. 1) do not seem to correlate with the number of grain-to-grain contacts (Figs 5a, b). The measured contact lengths show, however, a clear increase with decreasing grain size (Figs 5c, d). The Norne samples have a smaller grain size and are less cemented compared to the Kristin samples (Fig. 2) and each contact is, therefore, much smaller. Although the individual Norne grain contact lengths are smaller, there are many more of them so that the total amount (or sum) within a fixed area may become larger compared to the more extensively cemented coarser-grained Kristin samples. Figures 5e–h show that neither porosity nor velocity correlates with the contact-length measurements. Other combinations between the grain contact measurements and porosity, velocity or the elastic parameters listed in Table 1, did not show any systematic trends of significance.

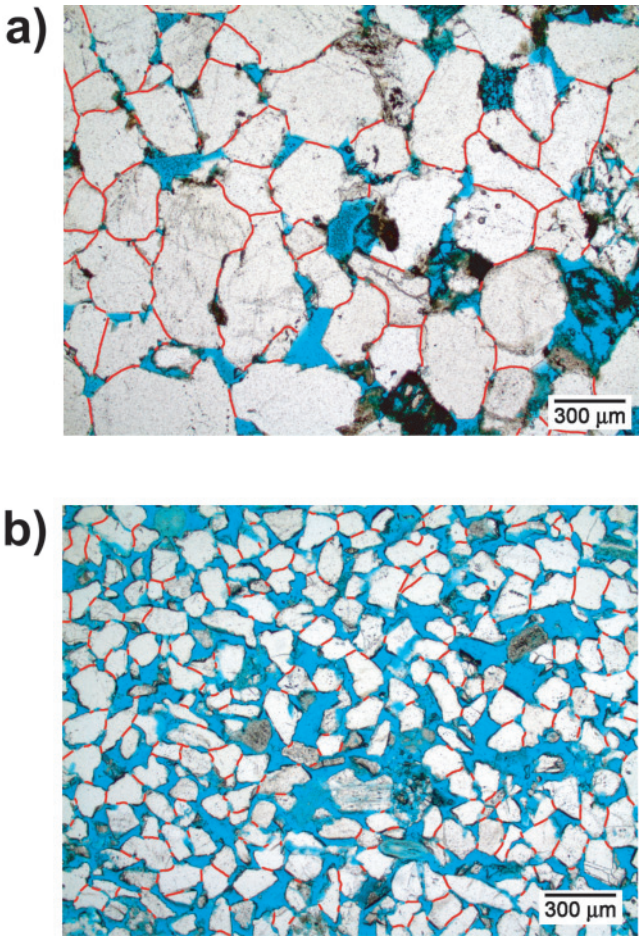

Fig. 2. Microscope image, under normal transmitted light, of the Garn Formation from (**a**) the Kristin sample set (4650 m depth) and (**b**) the Norne sample set (2623 m depth). Red lines represent the contact length between the grains; porosity is filled with blue epoxy.

Grain contact experiments (e.g. David *et al.* 1988) and contact theories, such as the Hertz (Love 1927), Mindlin (1949) and Digby (1981) models, often divide the contact parameter by the grain size to incorporate the important effect of grain-size variations. However, the contact measurements have been used directly, as explained in the discussion. Even if the contact-length parameter is divided by grain size, however, no new correlations are found.

Results from the laboratory velocity analysis are listed in Table 3. The ultrasonic velocity measurements show a significant variation from the log-derived velocities, especially in the Kristin samples, and no positive correlation was found (Figs 6a, b). No frequency corrections were performed on the laboratory-derived velocity data and generally higher ultrasonic velocities were as expected. The compressional ultrasonic velocity in the Norne samples increases about 250 m s^{-1} when measured under wet conditions (Table 3), mainly due to the bulk density increase when saturated. One sample (2641.15 m, lowest average grain size and highest contact length) shows, however, an increase of only 47 m s^{-1} in velocity when saturated, which is assumed to be the result of bad plug quality (e.g. fractures), problems/errors during the analysis or random variations resulting in large discrepancies because of the limited number of samples. The apparent negative correlation for the wet Norne samples in Figure 6b is, to a large extent, caused by this sample and the correlation is, therefore, disregarded. No significant correlation between the new contact-length data and the ultrasonic velocities in the Kristin samples is observed (Fig. 6c). A positive correlation with the ultrasonic shear velocity for the Norne samples is, however, present (Fig. 6d), and seems too high (R=0.92 and 0.99) to be only a coincidence due to the limited number of samples tested. A weaker positive correlation between the dry compressional ultrasonic velocity and grain contact length for the Norne samples is also recognized (Fig. 6d). The wet compressional ultrasonic velocity from the Norne samples shows no correlation with contact length, mainly due to the one sample that partly failed when saturated, as explained earlier.

The cathodoluminescence SEM pictures (Fig. 7) make it possible to distinguish between clastic quartz grains and authigenic quartz cement. The individual quartz grains also display varying degrees of luminescence, mainly caused by different environmental conditions (e.g. temperature and chemical variations) during crystallization. Figure 7 shows that, from a 2D perspective, some of the grains were not in direct contact prior to cementation. It is possible, however, that these grains were in contact somewhere in the third dimension of the sample. As indicated by the double arrows (Fig. 7a) the quartz cement has generated new grain-to-grain contacts and made existing contacts significantly larger. All the cracked grains found in the deeply buried (4.6–4.7 km) Garn Fm. from the Kristin Field are completely cemented (Fig. 7). The cracks originated most likely during mechanical compaction, down to 2.5–3 km burial depth. In the shallower-buried (2.6–2.7 km) and less-cemented Norne

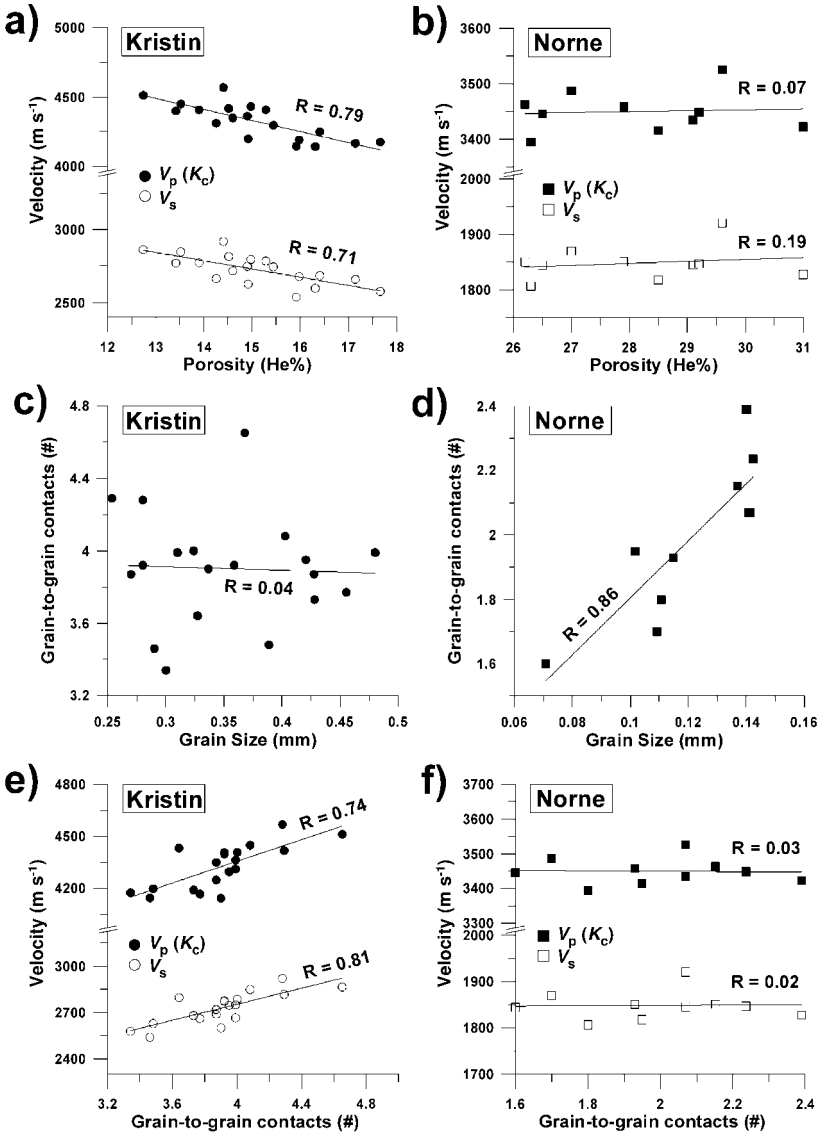

Fig. 3. (**a**) The samples from the Kristin well show decreasing velocity with increasing porosity, while (**b**) the Norne samples display no such correlation. (**c**) No correlation between grain size and number of grain-to-grain contacts exists in the extensively cemented Kristin samples. (**d**) In the less-cemented Norne samples a positive correlation is, however, found. (**e**) In the Kristin sample set the grain-to-grain contacts correlate with the compressional and shear velocity. (**f**) In the minor-cemented Norne samples no correlation or trend exists between velocity and grain-to-grain contacts. Note the broken axes.

samples, however, open cracks in individual grains can still be found (Fig. 8). Open or healed fractures cutting through more than one grain have not been observed in any of the studied samples from the Norne and Kristin fields.

DISCUSSION

Porosity, cementation and clay content

The number of grain-to-grain contacts and the size of existing contacts increase when sandstones undergo quartz cementation, basically as a result of cementation at existing grain contacts and because bridging occurs between grains previously not in contact (Fig. 7). Figures 3c, d support this statement, where a positive correlation between grain size and number of grain-to-grain contacts correlates in the only slightly cemented Norne samples, while in the deeply buried Kristin samples quartz cementation has increased the number of grain-to-grain contacts and no correlation with grain size, therefore, exists. Cementation also results in porosity reduction, however, which explains the correlation between number of grain-to-grain contacts and porosity in the Kristin samples (Fig. 4a). A negative correlation between porosity and velocity was found in the Garn Fm. from the Kristin sample set (Fig. 3a) and Figure 3e shows that grain-to-grain contacts also correlate with the velocities from the Kristin samples. Since quartz cementation has been shown to have a strong influence on porosity and number of grain-to-grain contacts in the Kristin samples (Figs 3a, e), it indirectly proves that quartz cementation is a critical factor with regard to velocity variations in the deeply buried Garn Fm. from the Kristin Field. The porosity, however, is also controlled by other factors, such as the intergranular volume prior to quartz cementation and the grain size.

The shallower-buried Garn Fm. from the Norne Field displayed no correlation between velocity and porosity (Fig. 3b). Figure 4d shows a negative correlation between porosity and clay content in the Norne samples, while in the deeper-buried Kristin sample set no clear correlation is observed (Fig. 4c). Ramm (1992) showed that primary sorting and clay content are critical factors that reduce porosity in sandstones down to a burial depth of 2.5–3 km, while, below 4 km, porosity loss is greatest in sandstones with low clay content due to extensive quartz cementation (Ramm & Bjørlykke 1994). The explanation is that, in deep reservoir sandstones, clay may appear as grain coatings preventing quartz cementation, thereby preserving porosity. The Garn Fm. in the Kristin well has been shown to have clay coatings of illite, illite/chlorite and chlorite (Storvoll

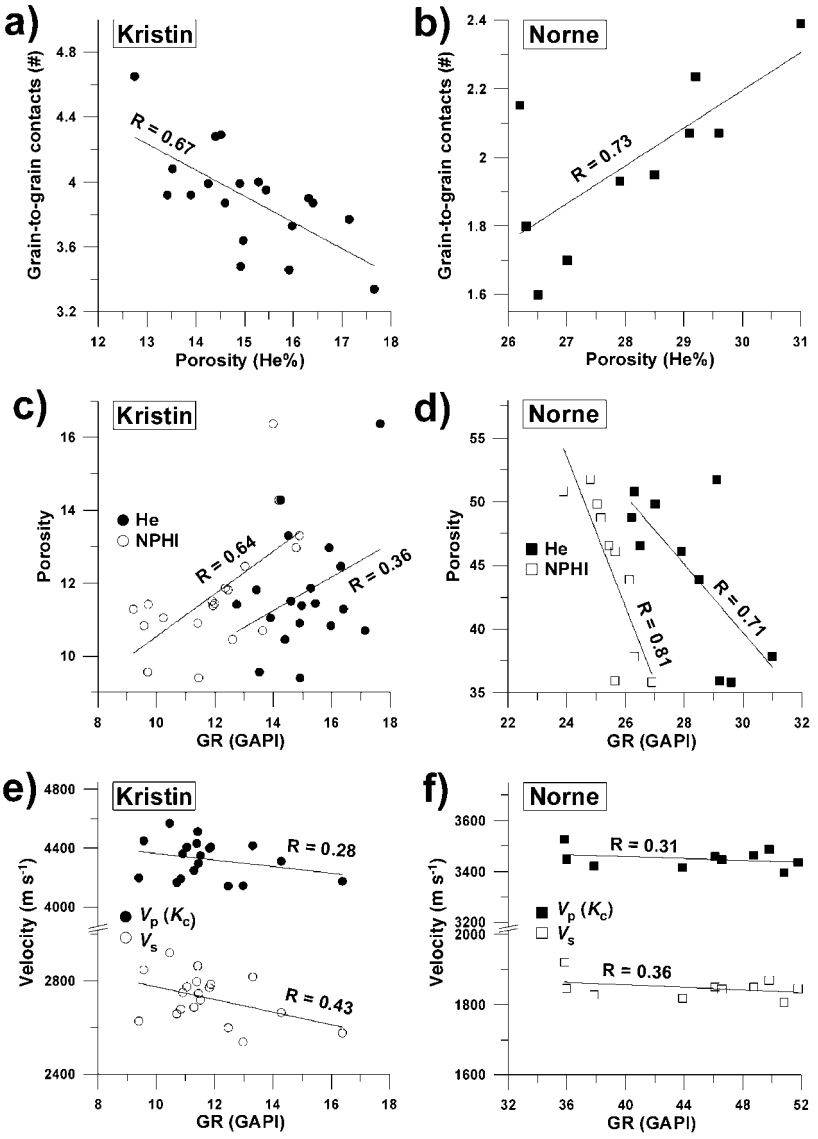

Fig. 4. (**a**) A negative trend is observed between porosity and number of grain contacts. (**b**) The Norne samples show a positive trend between porosity and number of grain-to-grain contacts, contrary to what was expected. (**c**) Clay content is often directly related to the gamma log response. The Kristin samples show no correlation or, at best, a weak positive trend when using neutron porosity, between clay content and porosity. NPHI is the neutron porosity, while He is the helium porosity. (**d**) In the Norne samples, however, increasing clay content results in decreasing porosity. (**e**, **f**) No correlation is observed between clay content and velocity for the Kristin and Norne samples.

et al. 2002), which might explain the weak positive trend in Figure 4c. The clay coatings affect quartz cementation and porosity, which controls velocity, but the total amount of clay in the Kristin samples will not directly affect the velocity (Fig. 4e) because the distribution of clay particles is more important than the volumetric amount of clay (Miller & Stewart 1990; Vernik & Nur 1992). In the Kristin samples, only a minor amount of clay is present and mainly located in the pore space or around grains as coatings. The importance of the structural position of clay in the rock also explains why no correlation was found between bulk volume of clay and velocity from the Norne samples (Fig. 4f). Including qualitative assessments and existing sand–clay models (e.g. Xu & White 1996) it is, however, likely that clay content is one of the most important parameters controlling velocity in the Norne samples.

Grain contact length

The measured grain contact parameter (contact length) is controlled by several geological factors: (1) grain size and shape and (2) type of contact (Fig. 1) – which are both mainly controlled by mechanical compaction and grain-to-grain pressure solution; and (3) cementation (located at/around the contacts), resulting from chemical diagenesis. In addition, many 'indirect' factors affect the final grain contact area, such as rate of burial, pore pressure, existence of clay coatings, pore fluid etc. The processes affecting and controlling the size of the grain contact area will often differ depending on the sample sets one is working with, which makes the contact area between grains difficult to predict even in seemingly similar samples before closer examination of cores and thin sections. The intention, however, when deciding to study grain contacts was not to find a predictive parameter to be used prior to drilling, but to try and understand the micro-mechanics related to elastic wave propagation in sandstones. The amount of time necessary to perform these types of analyses would also make it impractical to use on a more commercial basis.

Several studies have focused on the size of grain contacts and how grain contact area affects velocities (Digby 1981; Walton 1988; Anstey 1991; Dvorkin *et al.* 1991; Nur *et al.* 1991). The contact area measurements (contact-length) in the study here, however, did not give a clear correlation with the log-derived velocity (Fig. 5g), which questions the idea of a close relationship between grain contact area, rock stiffness and velocity. The present authors still think that variations in contact area have an influence on velocity, but that this is,

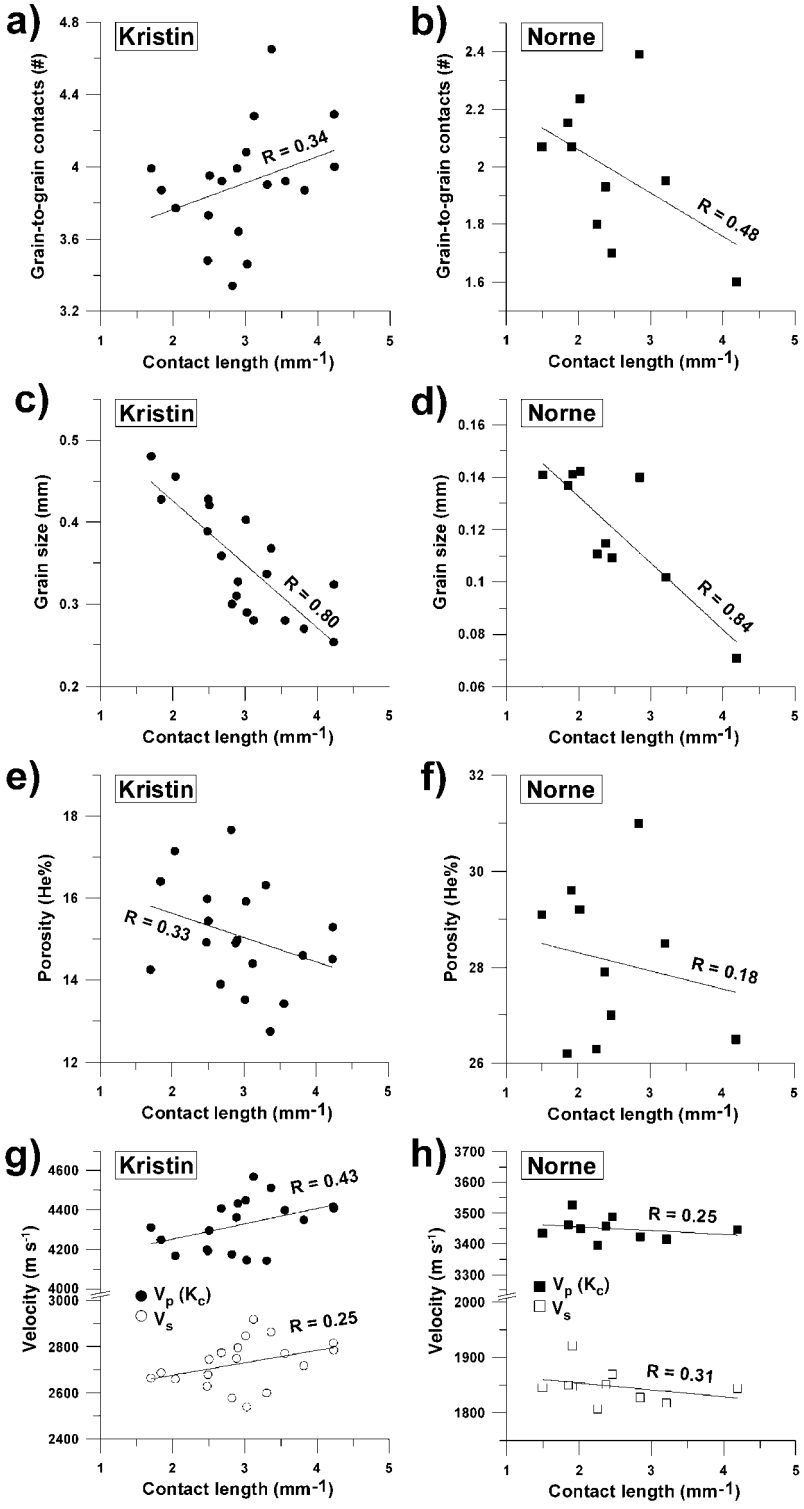

Fig. 5. (**a**, **b**) Contact-length measurements show no correlation with number of grain-to-grain contacts. (**c**, **d**) A clear correlation between contact-length measurement and grain size does, however, exist. (**e**–**h**) Neither porosity nor velocity gave any correlation with the contact-length measurements. The contact-length unit (mm^{-1}) is explained in the text. Note the broken axis.

perhaps, weaker and over a narrower diagenetic interval than previously assumed.

Since the sonic log represents averaged values of up to 30–60 cm of rock (depending of type of tool used in the logging process), small-scale variations observed in thin sections may not be recorded. He-porosity is, however, measured from cores – as is the number of grain-to-grain contacts – and both parameters correlate with log-derived data (Figs 3a, e). It is, therefore, unlikely that the absence of correlation between contact length and velocity (Fig. 5g) is only a result of scale. Perhaps the biggest problem is that real rocks are a three-dimensional medium, while thin sections show only a 2D image. Having thin sections of the same sample made at different angles could be a solution, but a simplification stating that what is seen in 2D will also be representative for the third dimension has been used instead. Since the work is in two dimensions, it must also be appreciated that the individual measurements cannot be considered as the diameter in an imaginary circular grain-to-grain contact. First of all one does not know if the sample cuts the contact at the middle (large

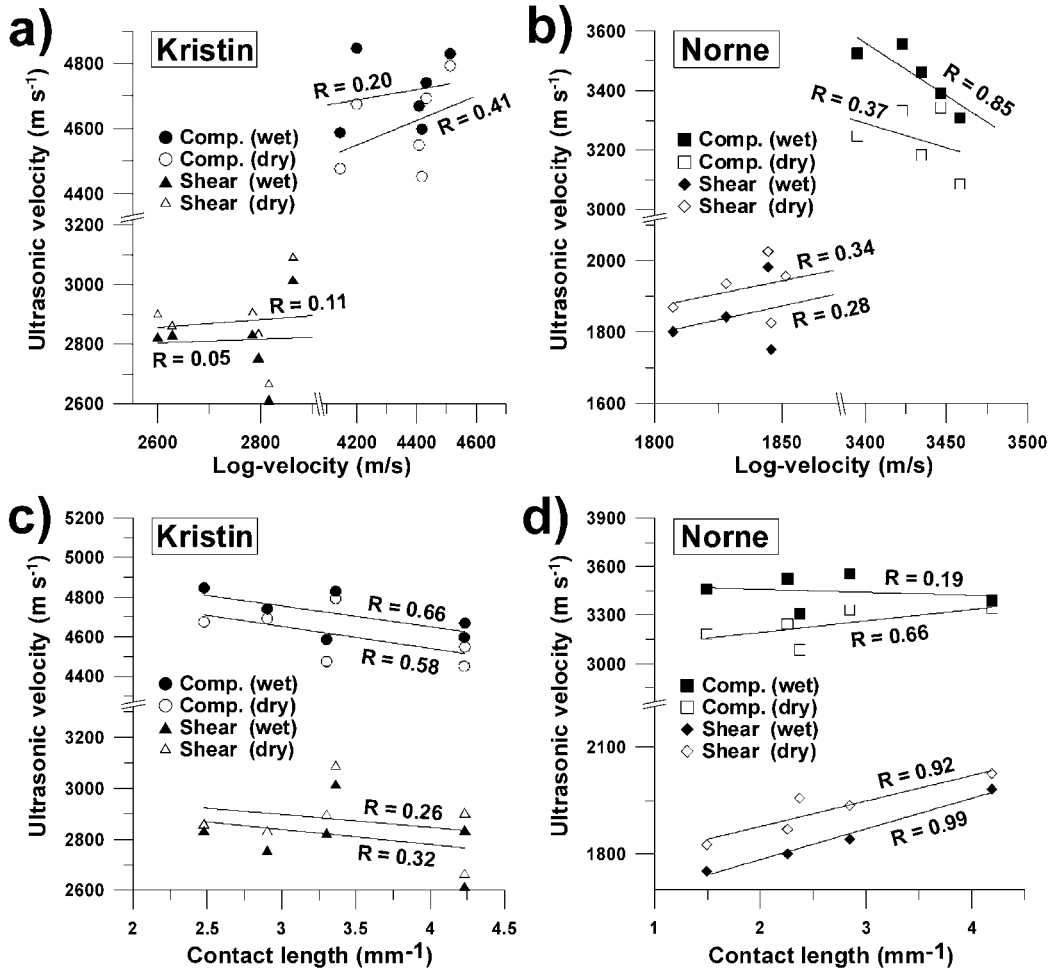

Fig. 6. Laboratory-derived ultrasonic velocity vs. log-derived velocity for (**a**) the Kristin and (the) the Norne samples. The apparent negative correlation for the wet compressional Norne measurements should be ignored, as explained in the text. One of the Norne samples failed during the wet shear velocities measurement and is, therefore, missing. Symbols indicated by 'Comp.' are the ultrasonic compressional velocity plotted against the log-derived compressional velocity ($V_p(K_c)$). Symbols called 'Shear' are the ultrasonic shear velocity plotted against the log-derived shear velocity (V_s). (**c**, **d**) The new contact-length measurements plotted against the laboratory-derived ultrasonic velocity measurements.

measurement) or at the edge (small measurement). In cemented samples it would also be wrong to think of the contacts as circular at all. This problem could be addressed by doing many measurements that, ultimately, are averaged and errors and uncertainties minimized or annulled. The drawback is the large amount of time necessary to analyse even a single thin section. It is important to remember that the contact-length parameter is thought to *represent* numerically the grain contact area, where high values correspond to large contacts and low values represent small contacts.

Despite the strong control that grain size has on contact length (Figs 5c, d), the authors are reluctant to divide the contact parameter by grain size since it will result in contact-length measurements that appear as if they were all measured from samples with similar grain size. This might seem an easy way to eliminate the effect of grain size when studying contact parameters, but it will also eliminate indirect grain size parameters that affect velocities in sandstones. One specific volume of cement precipitated at the grain contacts in a fine-grained sample, compared to a coarse-grained sample with otherwise similar mineralogy, does not necessarily mean that the variations in stiffness are entirely determined by the varying grain size. In real rocks grain size variations also lead to variations in the amount of polycrystalline grains, grain strength, type of grain contacts (Fig. 1), cracks and flaws in the crystal lattice, impurities etc. which may also contribute to variations in bulk stiffness. A closer examination of the indirect grain size parameters with regard to velocities should, at least, be considered before 'eliminating' the parameters by dividing the contact area measurements by grain size.

Ultrasonic core measurements

Because of scale-related problems, log-derived velocities involve uncertainties, but velocity measurements carried out in the laboratory are also subject to considerable uncertainties due to sample damage during and after coring (e.g. development of micro cracks), anisotropy and velocity dispersion. However, since the laboratory measurements are carried out on plugs located at the same depth from where the thin sections are sampled, the intention was to see if the ultrasonic velocities (Table 3) would correlate with the contact measurements where the log-derived velocities gave no correlation.

Figures 6a, b show that no clear relationship between the laboratory- and log-derived velocities exists, which may partly be a result of scale between core and well-log data, uncertainties during the laboratory measurements and/or sample damage. Only the ultrasonic velocities from the Norne samples gave a significant correlation with the new contact-length measurements (Fig. 6d). As recognized in other publications (Winkler

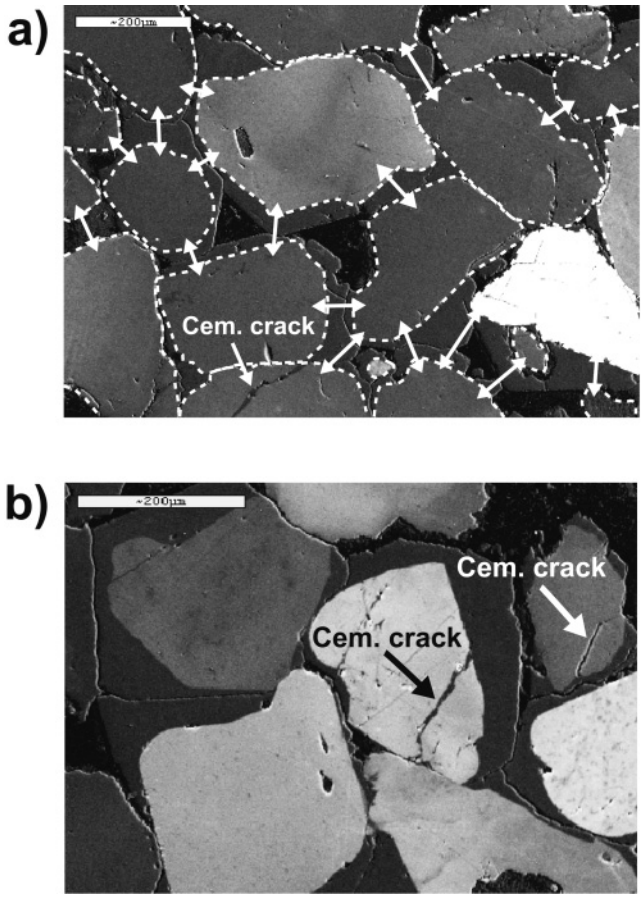

Fig. 7. Cathodoluminescence SEM pictures from the Kristin well (4686 m and 4679.8 m, respectively). The different shades of grey illustrate different degrees of luminescence, where clastic grains illuminate the most (light grey to white), while quartz cement (dark grey) and porosity (black) the least. (**a**) The stippled lines highlight the clastic grains, while the double arrows indicate grain-to-grain contacts originally absent (from a 2D perspective) prior to cementation. A cemented crack can also be observed in the lower part of the picture. (**b**) Cracks generated during mechanical compaction, but presently completely cemented.

1983; Bernabé *et al.* 1992; Vernik & Nur 1992; Dvorkin & Nur 1996), the early stages of chemical diagenesis and cementation result in an abrupt velocity increase because cement at the grain contacts stiffens the grain framework (Fig. 9). The shear velocity is a function of the rigidity in the sandstone, while the

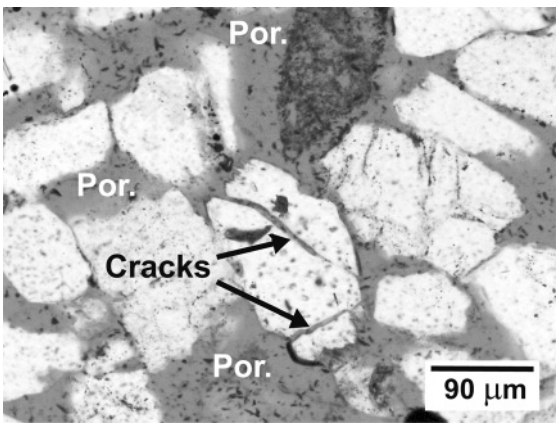

Fig. 8. Microscope image, under normal transmitted light, showing open cracks from a Norne sample (2674.25 m).

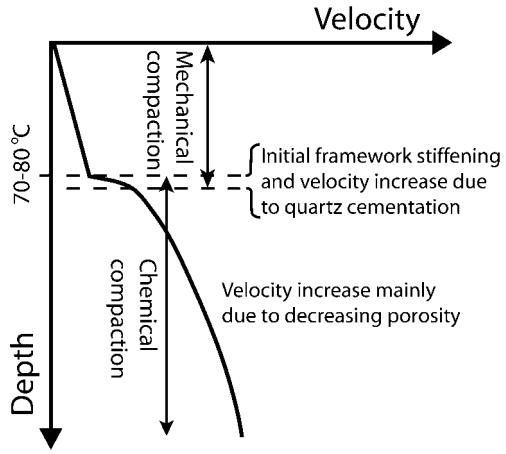

Fig. 9. The theoretical illustration shows velocity vs. depth for a reservoir sandstone in a normally subsiding basin. The initial grain-framework stiffening by cementation begins around 80–90°C and is marked by the upper stippled line. The second stippled line indicates a decreasing velocity/depth ratio where continued cementation will have less effect on the grain-framework stiffness and porosity controls the velocity variations.

compressional velocity is controlled by the rigidity and the bulk modulus (resistance to change of volume). Changes in rigidity will, therefore, affect the shear velocity more strongly than the compressional velocity. It is assumed that the early stages of grain-framework stiffening by cementation explain the positive correlation between the ultrasonic shear velocity and contact-length measurements (Fig. 6d), and that this rigidity increase may be too small to affect the ultrasonic compressional velocity as strongly as it has the shear velocity.

Based on the results in this study one can suggest that the grain contact area cannot be used to explain observed velocity variations during the entire burial interval of reservoir sandstones. The exception is during the initial grain-framework stiffening by cementation, where the contact-length parameter manages to reflect the ultrasonic shear velocity and dry compressional velocity variations (Fig. 6d). The framework stiffness increases rapidly due to initial cementation (starts around 70–80°C) and the stress per grain contact will decrease quickly. The results also show that after the initial stiffening of the grain framework, increasing grain contact area by further cementation does not seem to have a large effect on the velocity. Additional quartz cementation will primarily affect the porosity which, again, controls the velocity.

Cracks

In sandstones, velocities are very sensitive to the presence of thin cracks and crack-shaped or flat pores (Tao & King 1993; Xu & White 1995, 1996). The Garn Fm. in the Norne Field is located between 2.6 km and 2.7 km and quartz has started to precipitate, but some mechanical compaction may still be active. Broken grains, as a result of mechanical compaction, are present (Fig. 8), but coring, substantial pressure decrease during sampling and thin section preparation have also resulted in some of the cracked grains, which should be ignored when considering elasticity in the rock. Figure 7 shows that cracked grains caused by mechanical compaction in the Kristin samples have been completely cemented by quartz cement. The cracks are not cutting through the quartz overgrowth, which indicates that the crushing ended shortly after quartz cement started to precipitate (70–80°C).

Both experimental compaction of sand and observations from reservoir rocks show that grain fracturing is common in shallow (down to approximately 2.5–3 km) sandstone reservoirs (e.g. Chuhan *et al.* 2002). Cracks in sandstones are, however, also the first areas to become cemented because 'fresh' mineral surfaces without coatings or other minerals blocking the nucleation positions become exposed and cement will precipitate more easily (Xu & White 1995; Walderhaug 1996; Fisher & Knipe 1998). Mechanical compaction, crushing of grains and development of cracks (including micro cracks) end under normal circumstances after the onset of quartz cementation (70–80°C), as the overburden stress is distributed over more and larger contacts, and because the grain framework stiffens significantly as a result of the cementation. During continued subsidence, sandstones will tend to behave in a ductile manner and open fractures larger than the grain size are unlikely to develop except due to active faulting (Bjørlykke & Hoeg 1997).

One cannot exclude the possibility that cracked grains may have had some influence on velocity variations in the Norne samples (Fig. 8) but, in the deeply buried (4–5 km) extensively cemented Kristin samples, open cracks are not present and the cemented cracks will not affect the elasticity and, thus, the velocity, in the rock. Cracks or fractures are not considered common in reservoir sandstones buried below 3 km depth in a normal subsiding basin prior to drilling and production.

CONCLUSIONS

Petrographical analysis show that the size and number of grain-to-grain contacts increase during quartz cementation. Even small amounts of quartz cement near grain contacts will rapidly increase the grain framework stiffness and velocity in sandstones. The results also indicate that measurements of only the actual area between sand grains after the onset of quartz cementation can be used to explain velocity variations during the initial stiffening of the grain framework (Fig. 9). After the initial stiffening by quartz cementation, the stress per contact area is significantly reduced and increasing grain contact area by further cementation does not seem to correlate with the velocity. The velocity, however, has been shown to correlate with porosity in the samples from the Garn Formation from the Kristin Field (4.6–4.7 km). Quartz cementation is an important factor controlling porosity in deeply buried sandstones (>3 km), but porosity is also controlled by other factors, such as the intergranular volume prior to quartz cementation and grain size.

Quartz cementation is the main factor controlling porosity variations in the Garn Fm. from the Kristin Field (4.6–4.7 km) and is, therefore, essential with regard to the sonic velocity. The number of grain-to-grain contacts, porosity, velocity and the gamma-ray log in the shallower Norne samples (2.6–2.7 km) indicate that clay content is a critical parameter with regard to the velocity variations but, since it is the structural position of clay that is important and not the bulk volume, the relationship is difficult to quantify. Only small amounts of quartz cement are present in the Garn Fm. from the Norne Field (reservoir temperature of 98°C), which is undergoing the very beginning of grain framework stiffening. The positive correlation between the contact area (grain contact-length measurements) and the ultrasonic velocity is a direct result of the location of the Norne samples in this specific diagenetic interval, representing the end of mechanical compaction and beginning of chemical compaction (Fig. 9).

In the deeply buried Garn Fm. from the Kristin well all the cracked grains are thoroughly cemented and will not affect the sonic velocity. The healed cracks do not cut through the quartz overgrowth, indicating that the crushing ended shortly after quartz cement started to precipitate (70–80°C). In general, open cracks are considered rare in deeply buried (>3 km) reservoir rocks in a normally subsiding basin prior to drilling and production due to continued quartz cementation. In the shallower Norne samples only a few grains with open fractures were observed. It is, however, uncertain if and how these fractures have influenced the velocity.

This study was supported by VISTA, a research co-operation between the Norwegian Academy of Science and Letters and Statoil ASA. Statoil is also acknowledged for providing well logs, fluid data and other information necessary to complete this project. The authors would like to thank Lars Wensås for providing the ultrasonic velocity measurements, which were carried out at the Center for Rock Physics, University of Oklahoma (USA). Olav Walderhaug is acknowledged for helpful discussions and for providing the thin sections. Finally, the authors wish to thank Sverre Planke, Tor Arne Johansen, Paul Nadeau and Ivar Brevik for valuable suggestions, which improved on earlier versions of the manuscript.

REFERENCES

Anstey, N.A. 1991. Velocity in thin section. *First Break,* **9**, 449–457.

Batzle, M. & Wang, Z. 1992. Seismic Properties of Pore Fluids. *Geophysics,* **57**, 1396–1408.

Bernabé, Y., Fryer, D. & Hayes, J. 1992. The effect of cement on the strength of granular rocks. *Geophysical Research Letters,* **19**, 1511–1514.

Bjørlykke, K. & Hoeg, K. 1997. Effects of burial diagenesis on stresses, compaction and fluid flow in sedimentary basins. *Marine and Petroleum Geology,* **14**, 267–276.

Bjørlykke, K., Aagaard, P., Dypvik, H., Hastings, D.S. & Harper, A.S. 1986. Diagenesis and reservoir properties of Jurassic sandstones from the Haltenbanken area, offshore Mid Norway. *In:* Spencer, A.M. (ed.) *Habitat of Hydrocarbons on the Norwegian Continental Shelf.* Graham& Trotman, London, 275–286.

Bjørkum, P.A., Oelkers, E., Nadeau, P., Walderhaug, O. & Murphy, W. 1998. Porosity prediction in quartzose sandstones as a function of time, temperature, depth, stylolite frequency, and hydrocarbon saturation. *American Association of Petroleum Geologists Bulletin,* **82**, 637–648.

Chuhan, F.A., Kjeldstad, A., Bjørlykke, K. & Hoeg, K. 2002. Porosity loss in sand by grain crushing – experimental evidence and relevance to reservoir quality. *Marine and Petroleum Geology,* **19**, 39–53.

David, C., Menendez, B. & Bernabe, Y. 1988. The mechanical behaviour of synthetic sandstone with varying brittle cement content. *International Journal of Rock Mechanics and Mining Sciences,* **35**, 759–770.

Digby, P.J. 1981. The effective elastic moduli of porous granular rocks. *Journal of Applied Mechanics,* **48**, 803–808.

Dvorkin, J. & Nur, A. 1996. Elasticity of high-porosity sandstones: Theory for two North Sea data sets. *Geophysics,* **61**, 1363–1370.

Dvorkin, J., Mavko, G. & Nur, A. 1991. The Effect of Cementation on the Elastic Properties of Granular Material. *Mechanics of Materials,* **12**, 207–217.

Dvorkin, J., Nur, A. & Yin, H.Z. 1994. Effective Properties of Cemented Granular-Materials. *Mechanics of Materials,* **18**, 351–366.

Ehrenberg, S.N. 1990. Relationship between diagenesis and reservoir quality in sandstones of the Garn Formation, Haltenbanken, mid-Norwegian continental shelf. *American Association of Petroleum Geologists Bulletin,* **74**, 1538–1558.

Fisher, Q.J. & Knipe, R.J. 1998. Fault sealing processes in siliciclastic sediments. *In:* Jones, G., Fisher, Q.J. & Knipe, R.J. (eds) *Faulting, fault sealing and fluid flow in hydrocarbon reservoirs.* Geological Society, London, Special Publications, **147**, 117–134.

Han, D.H., Nur, A. & Morgan, D. 1986. Effects of porosity and clay content on wave velocities in sandstones. *Geophysics,* **51**, 2093–2107.

Klimentos, T. 1991. The effects of porosity–permeability–clay content on the velocity of compressional waves. *Geophysics,* **56**, 1930–1939.

Lo, T.W., Coyner, K.B. & Toksöz, M.N. 1986. Experimental-Determination of Elastic-Anisotropy of Berea Sandstone, Chicopee Shale, and Chelmsford Granite. *Geophysics,* **51**, 164–171.

Love, A.E.H. 1927. *Treatise on the mathematical theory of elasticity.* Cambridge University Press.

Mavko, G., Chan, C. & Mukerji, T. 1995. Fluid substitution: Estimating changes in Vp without knowing Vs. *Geophysics,* **60**, 1750–1755.

McCormack, M.D., Justice, M.G. & Sharp, W.W. 1985. A stratigraphic interpretation of shear and compressional wave seismic data for the Pennsylvanian Morrow Formation of southeastern New Mexico. *In:* Berg,

O.R. & Woolverton, D.G. (eds) *Seismic stratighaphy II; an intergrated approach to hydrocarbon exploration*. American Association of Petroleum Geologists, Tulsa, OK, 225–239.
Miller, S.L.M. & Stewart, R.R. 1990. Effects of lithology, porosity and shaliness on P- and S-wave velocities from sonic logs. *Canadian Journal of Exploration Geophysics,* **26**, 94–103.
Mindlin, R.D. 1949. Compliance of elastic bodies in contact. *Journal of Applied Mechanics,* **16**, 259–268.
Murphy, W., Winkler, K. & Kleinberg, R. 1986. Acoustic relaxation in sedimentary rocks: Dependence on grain contacts and fluid saturation. *Geophysics,* **51**, 757–766.
Nur, A. & Simmons, G. 1969. Stress-induced velocity anisotropy in rock – an experimental study. *Journal of Geophysical Research,* **74**, 6667–6674.
Nur, A. & Wang, Z.J. 1989. *Seismic and acoustic velocities in reservoir rocks*. Society of Exploration Geophysicists, Tulsa, Oklahoma.
Nur, A., Marion, D. & Yin, H. 1991. Wave velocities in sediments. *In:* Hovem, J.M., Richardson, M.D. & Stoll, R.D. (eds) *Shear waves in marine sediments; proceedings*. Kluwer, Dordrecht, 131–140.
Ramm, M. 1992. Porosity Depth Trends in Reservoir Sandstones – Theoretical-Models Related to Jurassic Sandstones Offshore Norway. *Marine and Petroleum Geology,* **9**, 553–567.
Ramm, M. & Bjørlykke, K. 1994. Porosity Depth Trends in Reservoir Sandstones – Assessing the Quantitative Effects of Varying Pore-Pressure, Temperature History and Mineralogy, Norwegian Shelf Data. *Clay Minerals,* **29**, 475–490.
Schreiber, E., Anderson, O.L. & Soga, N. 1973. *Elastic constants and their measurement*. McGraw-Hill, New York.
SigmaScan Pro4. 1995. http://www.spssscience.com.
Storvoll, V., Bjørlykke, K., Karlsen, D. & Saigal, G. 2002. Porosity preservation in reservoir sandstones due to grain-coating illite: a study of the Jurassic Garn Formation from the Kristin and Lavrans fields, offshore Mid-Norway. *Marine and Petroleum Geology,* **19**, 767–781.
Tao, G. & King, M.S. 1993. Porosity and pore structure from acoustic well logging data. *Geophysical Prospecting,* **41**, 435–451.
Taylor, J.M. 1950. Pore-space reduction in sandstones. *American Association of Petroleum Geologists Bulletin,* **34**, 701–716.
Vernik, L. 1998. Acoustic velocity and porosity systematics in siliciclastics. *The Log Analyst,* **39**, 27–35.
Vernik, L. & Nur, A. 1992. Petrophysical classification of siliciclastics for lithology and porosity prediction from seismic velocities. *American Association of Petroleum Geologists Bulletin,* **76**, 1295–1309.
Walderhaug, O. 1994. Precipitation rates for quartz cement in sandstones determined by fluid-inclusion microthermometry and temperature-history modeling. *Journal of Sedimentary Research Section A: Sedimentary Petrology and Processes,* **64**, 324–333.
Walderhaug, O. 1996. Kinetic modeling of quartz cementation and porosity loss in deeply buried sandstone reservoirs. *American Association of Petroleum Geologists Bulletin,* **80**, 731–745.
Walderhaug, O. 2000. Modeling quartz cementation and porosity in Middle Jurassic Brent Group sandstones of the Kvitebjorn Field, northern North Sea. *American Association of Petroleum Geologists Bulletin,* **84**, 1325–1339.
Walton, K. 1988. Wave propagation within random packings of spheres. *Geophysical Journal of the Royal Astronomical Society,* **92**, 89–97.
Wang, Z. 2000. Velocity–Density Relationships in Sedimentary Rocks. *In:* Wang, Z. & Nur, A. (eds) *Seismic and acoustic velocities in reservoir rocks*. Society of Exploration Geophysicists, Tulsa, Oklahoma, 258–268.
Wilkens, R., Simmons, G. & Caruso, L. 1984. The ratio Vp / Vs as a discriminant of composition for siliceous limestones. *Geophysics,* **49**, 1850–1860.
Winkler, K.W. 1983. Contact stiffness in granular porous materials: comparison between theory and experiment. *Geophysical Research Letters,* **10**, 1073–1076.
Wyllie, M., Gregory, A. & Gardner, L. 1956. Elastic wave velocities in heterogeneous and porous media. *Geophysics,* **21**, 41–70.
Wyllie, M., Gregory, A. & Gardner, G. 1958. An experimental investigation of factors affecting elastic wave velocities in porous media. *Geophysics,* **23**, 400.
Xu, S. & White, R.E. 1995. A new velocity model for clay–sand mixtures. *Geophysical Prospecting,* **43**, 91–118.
Xu, S. & White, R.E. 1996. A physical model for shear-wave velocity prediction. *Geophysical Prospecting,* **44**, 687–717.

Received 14 July 2003; revised typescript accepted 10 May 2004.